

# Interrelationship between small strain modulus $G_0$ and operative modulus

P. Monaco, S. Marchetti & G. Totani

*University of L'Aquila, Italy*

D. Marchetti

*Studio Prof. Marchetti, Rome, Italy*

**ABSTRACT:** This paper presents experimental diagrams constructed using same-depth values of the small strain modulus  $G_0$  and of the working strain modulus (constrained modulus)  $M$  determined by seismic dilatometer (SDMT) at 34 different sites in a variety of soil types, in order to investigate the interrelationship between the two moduli. The ratio  $G_0/M$  is plotted as a function of the DMT horizontal stress index  $K_D$  (stress history) and of the DMT material index  $I_D$  (indicative of clay, silt or sand). Such experimental diagrams offer some elements of reply to the questions: (1) Is it feasible, as sometimes suggested, to estimate the *operative modulus* as  $G_0$  divided by a constant? (2) Is it feasible, for a seismic classification, to use  $s_u$  or  $N_{SPT}$  as a substitute for  $V_S$  – when  $V_S$  has not been measured? Lines of research on the possible use of SDMT for deriving the in situ  $G$ - $\gamma$  decay curves are also outlined.

## 1 INTRODUCTION

The seismic dilatometer (SDMT) is the combination of the traditional "mechanical" Flat Dilatometer (DMT) introduced by Marchetti (1980) with a seismic module placed above the DMT blade. The SDMT module is a probe outfitted with two receivers, spaced 0.5 m, for measuring the shear wave velocity  $V_S$ . From  $V_S$  the small strain shear modulus  $G_0$  may be determined using the theory of elasticity. Motivations of the combined probe:

- $V_S$  and  $G_0$  are at the base of any seismic analysis.
- The  $G$ - $\gamma$  decay curves of stiffness with strain level are an increasingly requested input in seismic analyses and, in general, in non linear analyses.
- Increasing demand for liquefiability evaluations.
- Seismic site classification using directly  $V_S$  rather than the SPT blow count  $N_{SPT}$  or the undrained shear strength  $s_u$ .
- Availability of the usual DMT results (e.g. constrained modulus  $M_{DMT}$ ) for common design applications (e.g. settlement predictions).

The SDMT equipment and test procedure are briefly described in the paper. Comments on SDMT results and applications can be found in previous papers, in particular in Marchetti et al. (2008).

This paper is focused, essentially, on the experimental interrelationships between the small strain shear modulus  $G_0$  and the operative (working strain) constrained modulus  $M_{DMT}$ , investigated by use of

SDMT results obtained in the period 2004-2007 from a large number of tests at 34 sites, in a variety of soil types.

It must be emphasized the well known notion that, while the small strain shear modulus is unique, the *operative modulus* varies with strain. Hence, in theory, such comparison is impossible. However the term *operative modulus* sounds very familiar to practicing engineers, because they use it very often in design and would find useful methods providing even rough estimates of it. The price to pay is to accept (non negligible) approximation in the definition of the *operative modulus*, which however maybe still useful in practice, in view of the often very large errors in estimating such modulus.

## 2 THE SEISMIC DILATOMETER (SDMT)

The seismic dilatometer (SDMT) is the combination of the standard DMT equipment with a seismic module for measuring the shear wave velocity  $V_S$ .

Initially conceived for research, the SDMT is gradually entering into use in current site investigation practice. The test is conceptually similar to the seismic cone (SCPT). First introduced by Hepton (1988), the SDMT was subsequently improved at Georgia Tech, Atlanta, USA (Martin & Mayne 1997, 1998, Mayne et al. 1999). A new SDMT system (Fig. 1) has been recently developed in Italy.

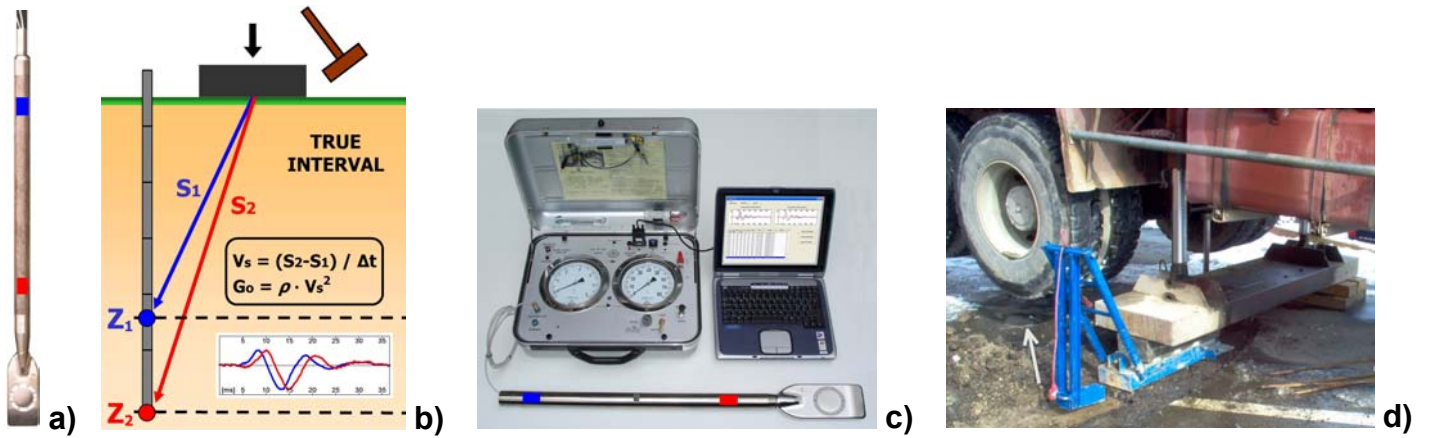


Figure 1. (a) DMT blade and seismic module. (b) Schematic layout of the seismic dilatometer test. (c) Seismic dilatometer equipment. (d) Shear wave source at the surface.

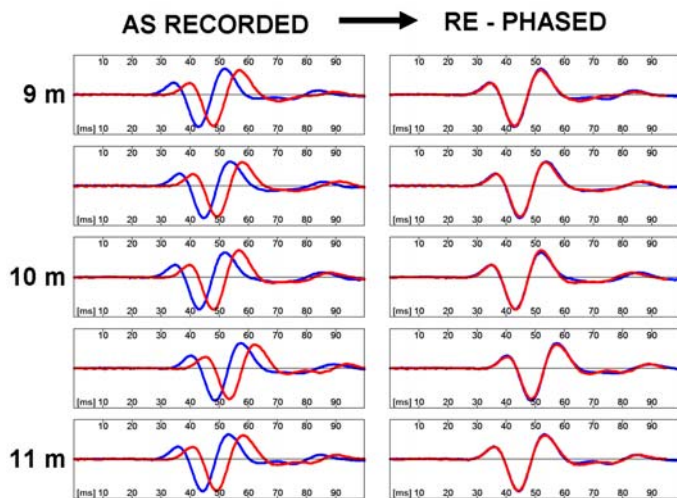


Figure 2. Example of seismograms obtained by SDMT at the site of Fucino (Italy)

The seismic module (Fig. 1a) is a cylindrical element placed above the DMT blade, outfitted with two receivers spaced 0.5 m. The signal is amplified and digitized at depth. The *true-interval* test configuration with two receivers avoids possible inaccuracy in the determination of the "zero time" at the hammer impact, sometimes observed in the *pseudo-interval* one-receiver configuration. Moreover, the couple of seismograms recorded by the two receivers at a given test depth corresponds to the same hammer blow and not to different blows in sequence, which are not necessarily identical. Hence the repeatability of  $V_S$  measurements is considerably improved (observed  $V_S$  repeatability  $\approx$  1-2 %).

$V_S$  is obtained (Fig. 1b) as the ratio between the difference in distance between the source and the two receivers ( $S_2 - S_1$ ) and the delay of the arrival of the impulse from the first to the second receiver ( $\Delta t$ ).  $V_S$  measurements are obtained every 0.5 m of depth.

The shear wave source at the surface (Fig. 1d) is a pendulum hammer ( $\approx$  10 kg) which hits horizontally a steel rectangular base pressed vertically against the

soil (by the weight of the truck) and oriented with its long axis parallel to the axis of the receivers, so that they can offer the highest sensitivity to the generated shear wave.

The determination of the delay from SDMT seismograms, normally carried out using the cross-correlation algorithm, is generally well conditioned, being based on the two seismograms – in particular the initial waves – rather than being based on the first arrival time or specific marker points in the seismogram. Figure 2 shows an example of seismograms obtained by SDMT at various test depths at the site of Fucino (it is a good practice to plot side-by-side the seismograms as recorded and re-phased according to the calculated delay).

Figure 3 (Fiumicino) is an example of the typical graphical format of the SDMT output. Such output displays the profile of  $V_S$  as well as the profiles of four basic DMT parameters – the material index  $I_D$  (soil type), the constrained modulus  $M$ , the undrained shear strength  $s_u$  and the horizontal stress index  $K_D$  (related to OCR) – obtained using current DMT correlations. (Information on the mechanical DMT, not described in this paper, can be found in the comprehensive report by the ISSMGE Technical Committee TC16 2001). It may be noted in Figure 3 that the repeatability of the  $V_S$  profile is very high, similar to the repeatability of the other DMT parameters.

$V_S$  measurements by SDMT have been validated by comparison with  $V_S$  measurements obtained by other in situ seismic tests at various research sites. As an example Figure 4 shows  $V_S$  comparisons at the research site of Fucino, Italy (NC cemented clay), extensively investigated at the end of the '80s. The profile of  $V_S$  obtained by SDMT in 2004 (Fig. 4) is in quite good agreement with  $V_S$  profiles obtained by SCPT, Cross-Hole and SASW in previous investigations (AGI 1991). Similar favourable comparisons are reported e.g. by Hepton (1988), McGillivray & Mayne (2004) and Mlynarek et al. (2006).

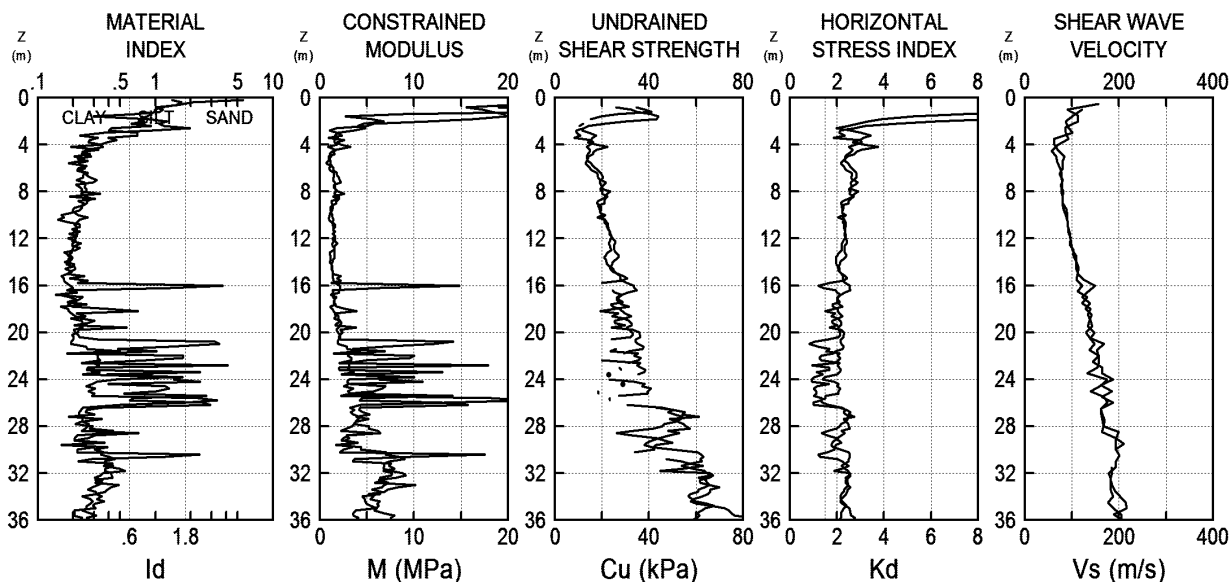


Figure 3. SDMT profiles from two parallel soundings at the site of Fiumicino (Italy)

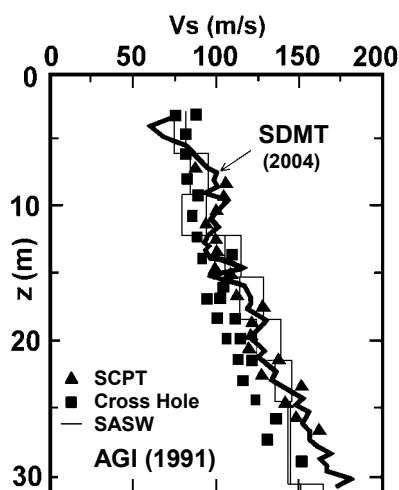


Figure 4. Comparison of  $V_S$  profiles obtained by SDMT and by SCPT, Cross-Hole and SASW (AGI 1991) at the research site of Fucino (Italy)

### 3 INTERRELATIONSHIPS BETWEEN EXPERIMENTAL $G_0$ AND $M_{DMT}$

The experimental diagrams presented in this section have been constructed using same-depth values of  $G_0$  (small strain shear modulus from  $V_S$ ) and  $M_{DMT}$  (constrained modulus from the usual DMT interpretation) determined by SDMT at 34 different sites, in a variety of soil types. The majority of the sites are in Italy, others are in Spain, Poland, Belgium and USA.

SDMT generates plentiful data points because each sounding routinely provides profiles of  $G_0$  and  $M_{DMT}$ , in addition to other parameters. Of the over 2000 data points available, only 800 high quality data points have been considered, relative to "uniform" one-m soil intervals where  $\log I_D$ ,  $K_D$ ,  $E_D$  (dilatometer modulus),  $M_{DMT}$ ,  $V_S$  all differ less than 30% from their average – used then to plot the data

points – to insure a proper match of the data. The DMT parameters have been calculated with the usual DMT interpretation formulae (see Marchetti 1980 or Table 1 in TC16 2001).

#### 3.1 Diagrams of the ratio $G_0/M_{DMT}$

The values of the ratio  $G_0/M_{DMT}$  (800 high quality data points from 34 sites) are plotted in Figure 5 as a function of the horizontal stress index  $K_D$  for clay (having material index  $I_D < 0.6$ ), silt ( $0.6 < I_D < 1.8$ ) and sand ( $I_D > 1.8$ ). Best fit equations are indicated for each soil type.

Recognizable trends in Figure 5 are: (a) The data points tend to group according to their  $I_D$  (soil type). (b)  $G_0/M_{DMT}$  is mostly in the range 0.5 to 3 in sand, 1 to 10 in silt, 1 to 20 in clay. (c) The widest range and the maximum variability of  $G_0/M_{DMT}$  are found in clay. (d) For all soils  $G_0/M_{DMT}$  decreases as  $K_D$  (related to OCR) increases.

Considerations emerging from the diagram:

(1) The ratio  $G_0/M$  varies in a wide range ( $\approx 0.5$  to 20 for all soils), hence it is far from being a constant. Its value is strongly dependent on multiple information, e.g. (at least) soil type and stress history. Therefore it appears next to impossible to estimate the operative modulus  $M$  by dividing  $G_0$  by a constant, as suggested by various Authors.

(2) If only mechanical DMT data are available, Figure 5 permits to obtain rough estimates of  $G_0$  (and  $V_S$ ) by use of the three parameters  $I_D$ ,  $K_D$ ,  $M$ . However there is no reason for not measuring directly  $V_S$  (e.g. by SCPT or SDMT).

(3) Figure 5 highlights the dominant influence of  $K_D$  on the ratio  $G_0/M$ . In case of non availability of  $K_D$ , all the experimental data points would cluster on the vertical axis. In absence of  $K_D$  – which reflects the *stress history* – the selection of the ratio  $G_0/M$

would be hopelessly uncertain. Hence as many as *three* informations, i.e.  $I_D$ ,  $K_D$ ,  $M$  (though only two independent), are needed to formulate rough estimates of  $G_0$  and  $V_S$ .

(4) In view of the consideration (3), the use of  $N_{SPT}$  or  $s_u$  alone as a substitute of  $V_S$  (when not measured) for the seismic classification of a site, as proposed e.g. by the Eurocode 8 and by various national codes, does not appear founded on a firm basis. In fact, if  $V_S$  is assumed to be the primary parameter for the classification of the site, then the possible substitute of  $V_S$  must be reasonably correlated to  $V_S$ . If three parameters ( $I_D$ ,  $K_D$ ,  $M$ ) are barely sufficient to obtain rough estimates of  $V_S$ , then the possibility to estimate  $V_S$  from only one parameter appears remote.

*Reason of plotting  $G_0/M$  ( $I_D$ ,  $K_D$ ) rather than  $G_0/E_D$  ( $I_D$ ,  $K_D$ ), i.e. reason of selecting a format not similar to the 1980 correlation  $M/E_D$  ( $I_D$ ,  $K_D$ ).*

The first attempt by the writers was to plot  $G_0/E_D$  ( $I_D$ ,  $K_D$ ) – where  $E_D$  is the dilatometer modulus, as many researchers had done before (Tanaka & Tanaka 1998, Sully & Campanella 1989, Baldi et al. 1989, Lunne et al. 1989, Hryciw 1990, Baldi et al. 1991, Cavallaro et al. 1999, Ricceri et al. 2001). The plot  $G_0/E_D$  was expected to contain less dispersion than the plot  $G_0/M$ , since the relationship  $M$  from  $E_D$  has its own variability. However it was found, contrary to expectations, that the degree of correlation in the  $G_0/E_D$  plot was lower (see Figure 6).

### 3.2 Diagrams of the ratio $G_{DMT}/G_0$

The diagrams in Figure 7 show the same experimental information as in Figure 5, but involve the additional modulus  $G_{DMT}$  derived from  $M_{DMT}$  using the formula of linear elasticity:

$$G = M / [2(1-\nu)/(1-2\nu)] \quad (1)$$

For an often assumed value  $\nu = 0.20$ :

$$G_{DMT} = M_{DMT} / 2.67 \quad (2)$$

All the  $G_{DMT}$  have been derived from  $M_{DMT}$  using Eq. 2, then the ratios  $G_{DMT}/G_0$  have been calculated too and plotted vs.  $K_D$  for clay, silt and sand (Fig. 7).

The reason of constructing Figure 7 is the following. The ratio  $G/G_0$  is the usual ordinate of the normalized  $G$ - $\gamma$  decay curve and has the meaning of a strain decay factor. Since  $M_{DMT}$  is a *working strain modulus* one might hypothesize that  $G_{DMT}$  is a *working strain shear modulus* too, in which case  $G_{DMT}/G_0$  could be regarded as the shear modulus decay factor at *working strains*.

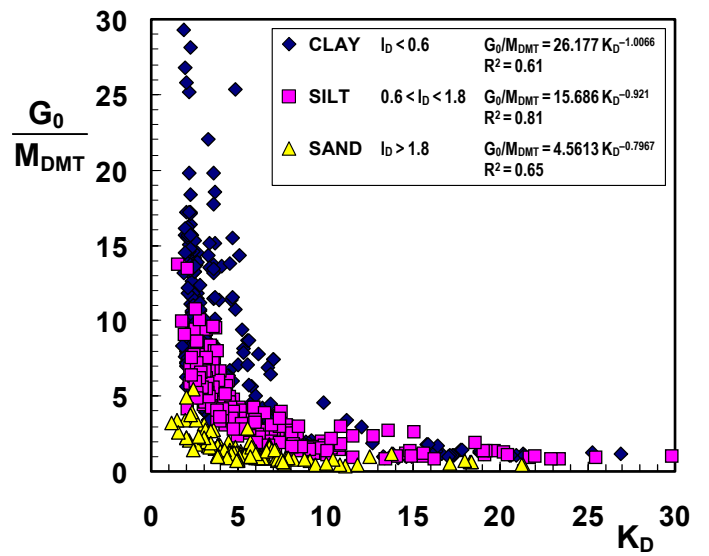


Figure 5. Ratio  $G_0/M_{DMT}$  vs.  $K_D$  (OCR) for various soil types

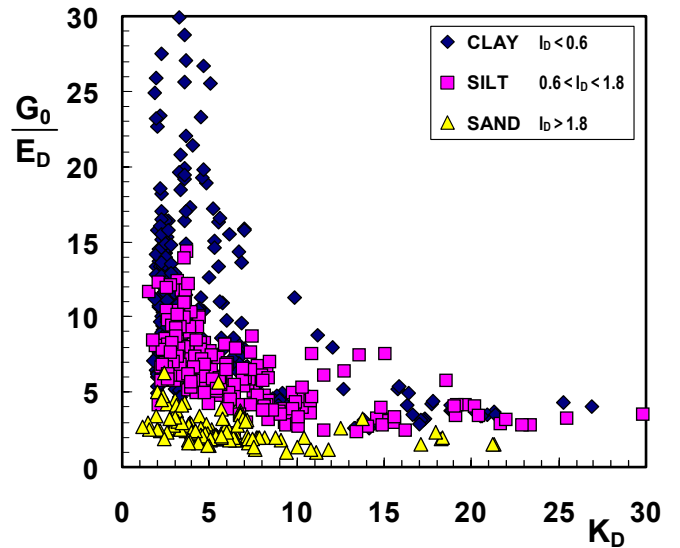


Figure 6. Ratio  $G_0/E_D$  vs.  $K_D$  for various soil types

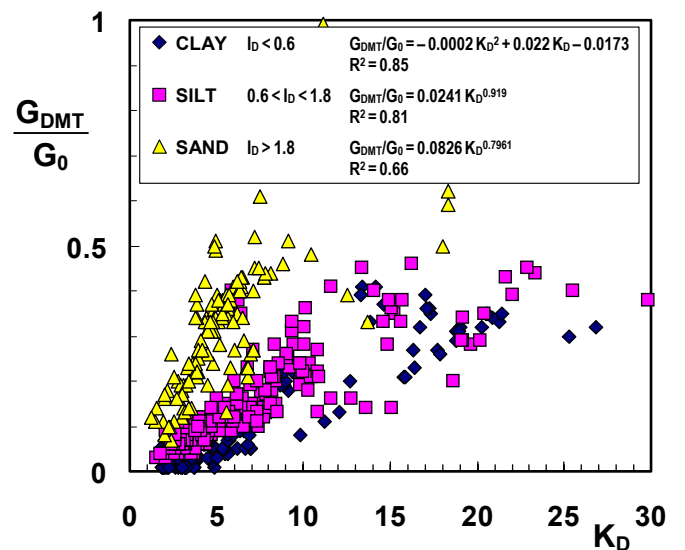


Figure 7. Decay ratio  $G_{DMT}/G_0$  vs.  $K_D$  for various soil types



It is emphasized that, at this stage, the legitimacy of using linear elasticity for deriving  $G_{DMT}$  from  $M_{DMT}$  (Eq. 2) and the assumption that  $G_{DMT}$  is a *working strain shear modulus* are only working hypotheses, likely more difficult to investigate than verifying that  $M_{DMT}$  is a *working strain constrained modulus* (the matter is discussed later in the paper). The very designation *working strain shear modulus* (or operative shear modulus) requires clarification.

Anyway, if the above hypotheses were acceptable, Figure 7 could provide, if  $I_D$  and  $K_D$  are known, rough estimates of the decay factor at *working strains*. If complete SDMT are available, then said rough estimates of the *decay factor* could be skipped and the factor could be obtained directly as the ratio between  $G_{DMT}$  derived from  $M_{DMT}$  (Eq. 2) and  $G_0$ .

Experimental information on the *decay factor* could possibly be of interest to researchers in the area of the  $G$ - $\gamma$  decay curves, who might find of interest experimental data indicating how fast  $G_0$  decays depending on soil type and stress history.

Trends emerging from Figure 7 are: (a) The  $G$  decay in sands is much less than in silts and clays. (b) The silt and clay decay curves are very similar. (c) For all soils the decay is maximum in the NC or lightly OC region (low  $K_D$ ).

#### 4 IN SITU $G$ - $\gamma$ DECAY CURVES BY SDMT

Research in progress investigates the possible use of the SDMT for deriving "in situ" decay curves of soil stiffness with strain level ( $G$ - $\gamma$  curves or similar).

Such curves could be tentatively constructed by fitting "reference typical-shape" laboratory curves (see Figure 8, where  $G$  is normalized to  $G_0$ ) through two points, both obtained by SDMT: (1) the *initial modulus*  $G_0$  from  $V_s$ , and (2) a *working strain modulus*  $G_{DMT}$  corresponding to  $M_{DMT}$  (Eq. 2).

To locate the second point it is necessary to know, at least approximately, the shear strain corresponding to  $G_{DMT}$ . Indications by Mayne (2001) locate the DMT moduli at an intermediate level of strain ( $\gamma \approx 0.05$ - $0.1\%$ ) along the  $G$ - $\gamma$  curve. Similarly Ishihara (2001) classified the DMT within the group of methods of measurement of soil deformation characteristics involving an intermediate level of strain ( $0.01$ - $1\%$ ). The above indications, to be supplemented by further investigations, could possibly help develop methods for deriving in situ  $G$ - $\gamma$  curves from SDMT.

Lines of research on this topic were first outlined by Lehane & Fahey (2004).

Lines of research currently under investigation (Marchetti et al. 2008) are:

(a) Enter the  $G_{DMT}/G_0$  ratios of Figure 7 in the vertical axis of "reference typical-shape"  $G$ - $\gamma$  curves recommended in the literature for the corresponding

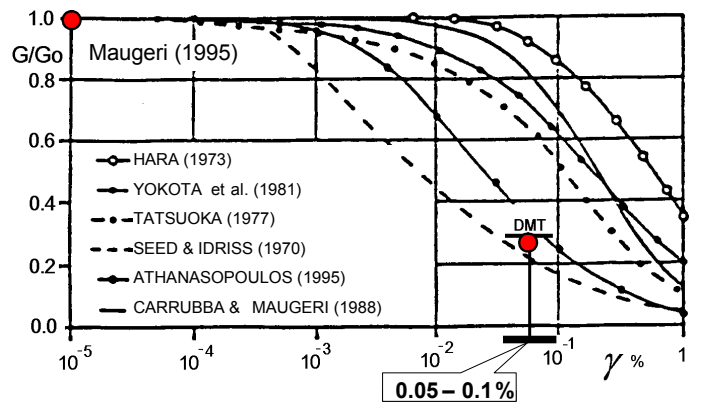


Figure 8. Tentative method for deriving  $G$ - $\gamma$  curves from SDMT

soil type. The range of abscissas of the intersection points with the  $G$ - $\gamma$  curves could possibly help to better define the shear strain corresponding to  $G_{DMT}$ .

(b) Develop a procedure for selecting the  $G$ - $\gamma$  curve, among the typical curves recommended in the literature, making use of  $I_D$  for choosing the band of curves recommended for the soil type (sand or silt or clay), and  $K_D$  (possibly  $G_0/M_{DMT}$  too) for selecting one curve in the band.

(c) Evaluate for each of the 800 data points in Figure 5 the settlement under a simple loading scheme using the simple linear analysis with input  $M_{DMT}$  (operation equivalent to converting a DMT investigation into a "virtual" load test). Then calculate the settlement by non linear analyses with  $G$ - $\gamma$  curves having variable rates of decay as input. By trial and error identify the  $G$ - $\gamma$  curve (originating in  $G_0$ ) producing agreement between the two predicted settlements. Consider such  $G$ - $\gamma$  curve reasonably correct and use it in the development of procedures for selecting the  $G$ - $\gamma$  curves from SDMT data.

#### 5 $M_{DMT}$ AS AN OPERATIVE OR WORKING STRAIN MODULUS

The possible use of the SDMT for deriving "in situ"  $G$ - $\gamma$  decay curves is heavily founded on the basic premise that  $M_{DMT}$  is as a reasonable estimate of the *operative* or *working strain modulus*, i.e. the modulus that, introduced into the linear elasticity formulae, predicts with acceptable accuracy the settlements under working loads. (The terms *operative modulus* and *working strain modulus* are considered synonyms and used interchangeably in this paper).

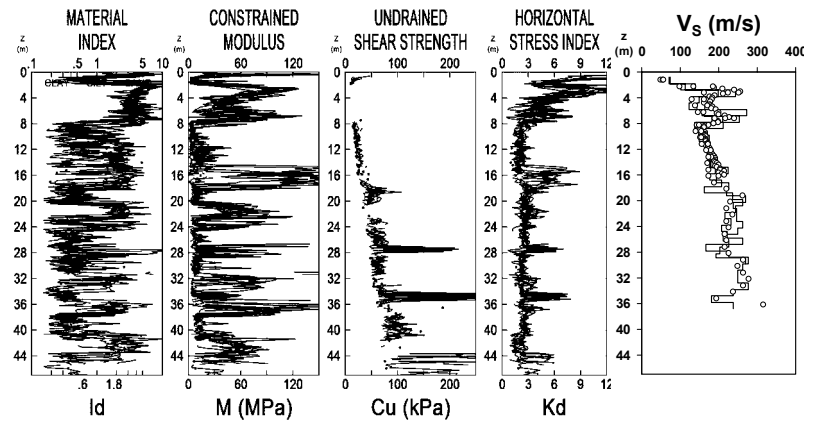
It is therefore considered appropriate to recall here the presently available evidence.

##### (a) Comparisons of surface settlements

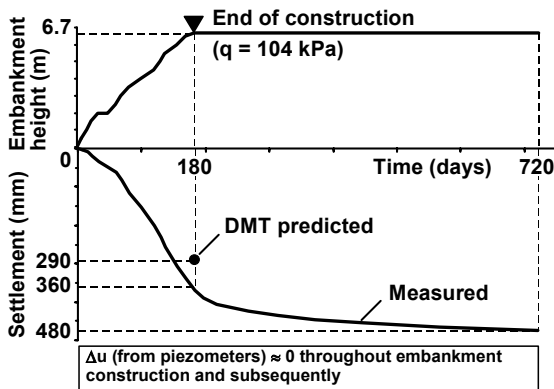
Schmertmann (1986) reported 16 case histories at various locations and for various soil types, with measured settlements ranging from 3 to 2850 mm.



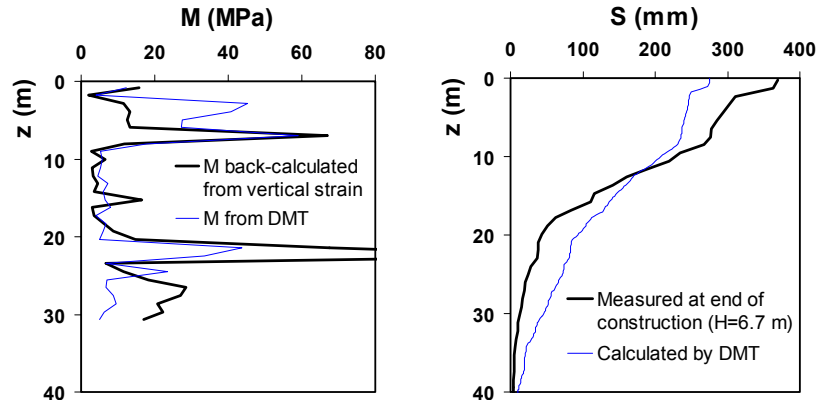
(a) Test embankment. Penetrometer truck for testing after construction.



(b) Superimposed profiles of all SDMT data



(c) Settlement vs. time at the center of the embankment and comparison of measured vs. DMT-predicted settlements at the end of construction



(d)  $M_{DMT}$  vs.  $M$  back-calculated from local  $\varepsilon_v$  measured at 1 m depth intervals under the center at the end of construction

(e) Observed vs. DMT-predicted settlement under the center at the end of construction

Figure 9. Venezia-Treporti Research Embankment. SDMT profiles. Predicted vs. observed moduli and settlements (Marchetti et al. 2006).

In most cases settlements from DMT were calculated using the Ordinary 1-D Method. The average ratio DMT-calculated/observed settlement was 1.18, with the value of the ratio mostly in the range 0.7 to 1.3 and a standard deviation of 0.38.

Monaco et al. (2006) reviewed numerous real-life well documented comparisons of DMT-predicted versus measured settlements. The average ratio DMT-calculated/observed settlement for all the cases reviewed by Monaco et al. (2006) is  $\approx 1.3$ , with an observed settlement within  $\pm 50\%$  from the DMT-predicted settlement.

The above settlements comparisons appear to support the assumption that  $M_{DMT}$  is a reasonable estimate of the constrained *working strain modulus*.

### (b) Comparisons of moduli

Even more direct, but rarely available, are data comparing  $M_{DMT}$  with moduli back-figured from local vertical strain measurements – by far more realistic and preferable for calibration or comparison purposes.

In 2002 a major research project, funded by the Italian Ministry of University and Scientific Research and by Consorzio Venezia Nuova, was undertaken by a consortium of three Italian Universities (Padova, Bologna and L'Aquila). A full-scale cylindrical heavily instrumented test embankment (40 m diameter, 6.7 m height, applied load 104 kPa – Fig. 9a) was constructed at the site of Venezia-Treporti, typical of the highly stratified, predominantly silty deposits of the Venezia lagoon (Fig. 9b). The loading history, the progression of the settlements and the drainage conditions – practically fully drained – are shown in Figure 9c.

A specific aim of the research was to obtain a profile of the observed 1-D operative modulus  $M$  under the center of the embankment. For this purpose a high precision sliding micrometer was used to accurately measure the *local* vertical strain  $\varepsilon_v$  at 1 m depth intervals.

$M$  values were back-calculated from local vertical strains  $\varepsilon_v$  in each 1 m soil layer as  $M = \Delta\sigma_v / \varepsilon_v$ , with vertical stress increments  $\Delta\sigma_v$  calculated at the mid-height of each layer by linear elasticity formulae

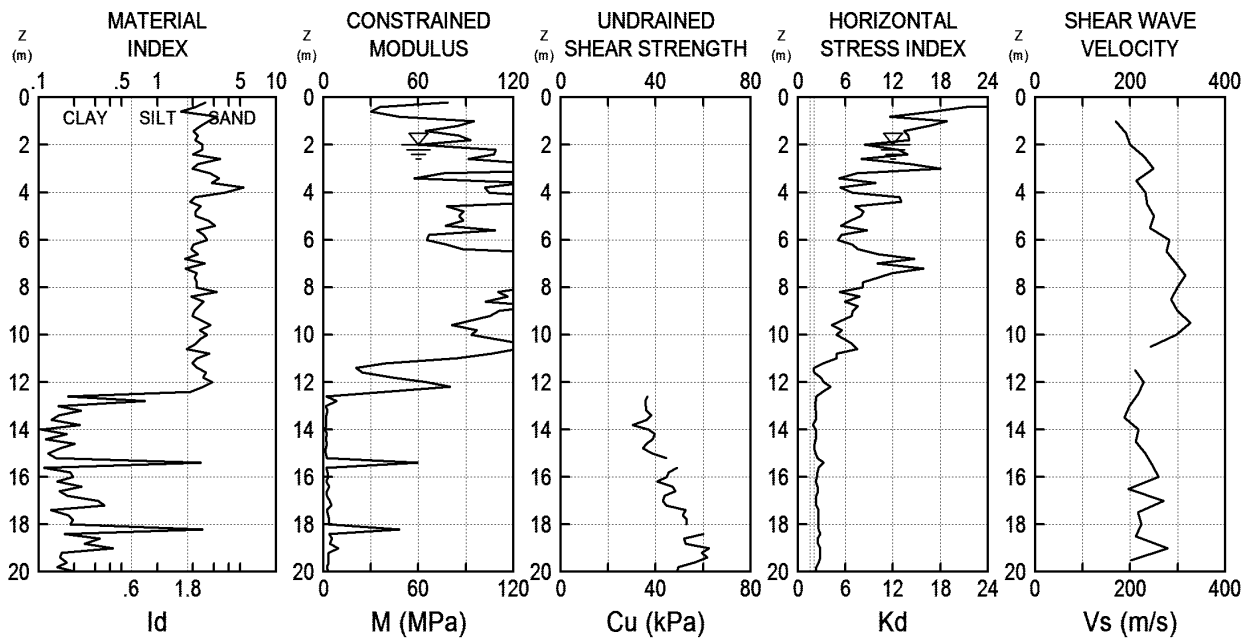


Figure 10. SDMT profiles at the site of Barcelona – El Prat Airport (Spain)

(approximation considered acceptable in view of the very low  $\varepsilon_h$ ). Figure 9d, which is believed to be one of the *most important results* of the Venezia-Treporti research, shows an overall satisfactory agreement between  $M_{DMT}$  and moduli back-figured from the test embankment performance, also considering the marked soil heterogeneity. Figure 9e compares the observed versus DMT-predicted settlements at each depth. Again the agreement is rather satisfactory, considering that the DMT predicted settlements were calculated using the simple linear 1-D conventional approach  $s = \Sigma (\Delta\sigma_v / M_{DMT}) \Delta H$ , where  $\Delta\sigma_v$  is calculated by Boussinesq linear elasticity formulae.

As to the surface settlements, the total settlement measured under the center of the embankment at the end of construction (180 days) was  $\approx 36$  cm (Fig. 9c). The settlement predicted by  $M_{DMT}$  using the 1-D approach (before knowing the results) was 29 cm. Hence the 29 cm predicted by DMT (which does not include secondary) are in good agreement with the 36 cm observed settlement (which includes some secondary during construction).

More details on the Venezia-Treporti research can be found in Marchetti et al. (2006), also containing numerous additional bibliographic references.

In conclusion also the Venezia-Treporti case-history supports the assumption that  $M_{DMT}$  is a reasonable estimate of the constrained *working strain modulus*.

## 6 DERIVABILITY OF THE OPERATIVE MODULUS $M$ FROM $G_0$

Figure 10 (Barcelona airport site) shows that at  $\approx 12$  m depth (transition from an upper stiff sand layer to a lower very soft clay layer) the modulus

$M_{DMT}$  exhibits a drastic drop, while  $V_S$  shows only a minor decrease. Hence  $G_0 = \rho V_S^2$  (even considering the power 2) is far from being proportional to the *working strain modulus*  $M$ .

Similar lack of proportionality, with variations of the ratio  $G_0/M_{DMT}$  often of one order of magnitude, has been observed at many sites (including Venezia, Figure 9d), suggesting that it is next to impossible (at least without local layer-specific correlations) to derive the *working strain modulus* by simply reducing the *small strain modulus* by a fixed percent factor (e.g. 50%, Simpson 1999).

On the other hand the poor correlability  $M$  to  $G_0$  was expected, since at small strains the soil tendency to dilate or contract is not active yet. Such tendency substantially affects the operative modulus  $M$ , but does not affect  $G_0$ . Said in a different way,  $M$  includes some stress history information,  $G_0$  does not (Powell & Butcher 2004). It may be noted that the high variability of the ratio  $G_0/M$  is already clearly expressed by Figure 5.

## 7 CONCLUSIONS

The seismic dilatometer SDMT provides routinely at each depth both a *small strain modulus* ( $G_0$  from  $V_S$ ) and *working strain modulus* (constrained modulus  $M_{DMT}$  – as indicated by numerous favourable real-life comparisons of DMT-predicted vs. measured settlements or moduli).

Based on a large number of results by SDMT, diagrams showing experimental interrelationships  $G_0 - M_{DMT}$  have been constructed. Figure 5 illustrates the most significant observed trends.

Figure 5 permits to obtain rough estimates of  $G_0$  (and  $V_S$ ) when  $V_S$  is not measured and only mechani-

cal DMT results are available ( $I_D$ ,  $K_D$ ,  $M$ ). Moreover Figure 5 indicates:

(1) Deriving the operative modulus  $M$  for settlement predictions from  $G_0$ , by dividing  $G_0$  by a fixed number (as suggested by various Authors), appears arduous. Often to drastic variations in the  $M$  profile correspond barely visible variations in the  $G_0$  profile. The ratio  $G_0/M$  varies in the wide range 0.5 to 20, hence it is far from being a constant, especially in clays and silts. Its value is strongly dependent on multiple information, e.g. soil type and stress history.

(2) To use only one information (e.g.  $N_{SPT}$  or  $s_u$ ) as a substitute of  $V_S$  (when not measured) for the seismic classification of a site, as suggested by various codes, appears of dubious validity.

Current research investigates the possible use of the SDMT for deriving "in situ" decay curves of soil stiffness with strain level, by fitting "reference  $G$ - $\gamma$  curves" through two points provided by SDMT at different strain levels: the *small strain* shear modulus  $G_0$  (from  $V_S$ ) and a *working strain* modulus corresponding to  $M_{DMT}$ .

## REFERENCES

- AGI. 1991. Geotechnical Characterization of Fucino Clay. *Proc. X ECSMFE*, Firenze, 1: 27-40.
- Baldi, G., Bellotti, R., Ghionna, V.N. & Jamiolkowski, M. 1991. Settlement of Shallow Foundations on Granular Soils. (a) Discussion. *J. Geotech. Engrg.*, 117(1): 72-175. ASCE.
- Baldi, G., Bellotti, R., Ghionna, V., Jamiolkowski, M. & Lo Presti, D.C.F. 1989. Modulus of Sands from CPT's and DMT's. *Proc. XII ICSMFE*, Rio de Janeiro, 1: 165-170.
- Cavallaro, A., Lo Presti, D.C.F., Mageri, M. & Pallara, O. 1999. Caratteristiche di deformabilità dei terreni da prove dilatometriche: analisi critica delle correlazioni esistenti. *Proc. XX Italian Geotech. Conf. CNG*, Parma: 47-53 (in Italian). Bologna: Pàtron.
- Hepton, P. 1988. Shear wave velocity measurements during penetration testing. *Proc. Penetration Testing in the UK*: 275-278. ICE.
- Hryciw, R.D. 1990. Small-Strain-Shear Modulus of Soil by Dilatometer. *J. Geotech. Engrg.*, 116(11): 1700-1716. ASCE.
- Ishihara, K. 2001. Estimate of relative density from in-situ penetration tests. In P.P. Rahardjo & T. Lunne (eds), *Proc. Int. Conf. on In Situ Measurement of Soil Properties and Case Histories*, Bali: 17-26.
- Lunne, T., Lacasse, S. & Rad, N.S. 1989. State of the Art Report on In Situ Testing of Soils. *Proc. XII ICSMFE*, Rio de Janeiro, 4: 2339-2403.
- Marchetti, S. 1980. In Situ Tests by Flat Dilatometer. *J. Geotech. Engrg. Div.*, 106(GT3): 299-321. ASCE.
- Marchetti, S., Monaco, P., Calabrese, M. & Totani, G. 2006. Comparison of moduli determined by DMT and backfigured from local strain measurements under a 40 m diameter circular test load in the Venice area. In R.A. Failmezger & J.B. Anderson (eds), *Proc. 2<sup>nd</sup> Int. Conf. on the Flat Dilatometer*, Washington D.C.: 220-230.
- Marchetti, S., Monaco, P., Totani, G. & Marchetti, D. 2008. In Situ Tests by Seismic Dilatometer (SDMT). In J.E. Laier, D.K. Crapps & M.H. Hussein (eds), *From Research to Practice in Geotechnical Engineering*, ASCE Geotech. Spec. Publ. No. 180 (honoring Dr. John H. Schmertmann): 292-311.
- Martin, G.K. & Mayne, P.W. 1997. Seismic Flat Dilatometer Tests in Connecticut Valley Varved Clay. *ASTM Geotech. Testing J.*, 20(3): 357-361.
- Martin, G.K. & Mayne, P.W. 1998. Seismic flat dilatometer in Piedmont residual soils. In P.K. Robertson & P.W. Mayne (eds), *Proc. 1<sup>st</sup> Int. Conf. on Site Characterization*, Atlanta, 2: 837-843. Rotterdam: Balkema.
- Mayne, P.W. 2001. Stress-strain-strength-flow parameters from enhanced in-situ tests. In P.P. Rahardjo & T. Lunne (eds), *Proc. Int. Conf. on In Situ Measurement of Soil Properties and Case Histories*, Bali: 27-47.
- Mayne, P.W., Schneider, J.A. & Martin, G.K. 1999. Small- and large-strain soil properties from seismic flat dilatometer tests. *Proc. 2<sup>nd</sup> Int. Symp. on Pre-Failure Deformation Characteristics of Geomaterials*, Torino, 1: 419-427.
- McGillivray, A. & Mayne, P.W. 2004. Seismic piezocone and seismic flat dilatometer tests at Treport. In A. Viana da Fonseca & P.W. Mayne (eds), *Proc. 2<sup>nd</sup> Int. Conf. on Site Characterization*, Porto, 2: 1695-1700. Rotterdam: Millpress.
- Młynarek, Z., Gogolik, S. & Marchetti, D. 2006. Suitability of the SDMT method to assess geotechnical parameters of post-flotation sediments. In R.A. Failmezger & J.B. Anderson (eds), *Proc. 2<sup>nd</sup> Int. Conf. on the Flat Dilatometer*, Washington D.C.: 148-153.
- Monaco, P., Totani, G. & Calabrese, M. 2006. DMT-predicted vs observed settlements: a review of the available experience. In R.A. Failmezger & J.B. Anderson (eds), *Proc. 2<sup>nd</sup> Int. Conf. on the Flat Dilatometer*, Washington D.C.: 244-252.
- Powell, J.J.M. & Butcher, A.P. 2004. Small Strain Stiffness Assessments from in Situ Tests. In A. Viana da Fonseca & P.W. Mayne (eds), *Proc. 2<sup>nd</sup> Int. Conf. on Site Characterization*, Porto, 2: 1717-1722. Rotterdam: Millpress.
- Ricceri, G., Simonini, P. & Cola, S. 2001. Calibration of DMT for Venice soils. In P.P. Rahardjo & T. Lunne (eds), *Proc. Int. Conf. on In Situ Measurement of Soil Properties and Case Histories*, Bali: 193-199.
- Schmertmann, J.H. 1986. Dilatometer to compute Foundation Settlement. *Proc. ASCE Spec. Conf. on Use of In Situ Tests in Geotechnical Engineering In Situ '86*, Virginia Tech, Blacksburg. ASCE Geotech. Spec. Publ. No. 6: 303-321.
- Simpson, B. 1999. Engineering needs. *Proc. 2<sup>nd</sup> Int. Symp. Pre-Failure Deformation Characteristics of Geomaterials*, Torino.
- Sully, J.P. & Campanella, R.G. 1989. Correlation of Maximum Shear Modulus with DMT Test Results in Sand. *Proc. XII ICSMFE*, Rio de Janeiro, 1: 339-343.
- Tanaka, H. & Tanaka, M. 1998. Characterization of Sandy Soils using CPT and DMT. *Soils and Foundations*, 38(3): 55-65.
- TC16. 2001. The Flat Dilatometer Test (DMT) in Soil Investigations - A Report by the ISSMGE Committee TC16. May 2001, 41 pp. Reprinted in R.A. Failmezger & J.B. Anderson (eds), *Proc. 2<sup>nd</sup> Int. Conf. on the Flat Dilatometer*, Washington D.C.: 7-48.